Air-sea gas exchange in a seagrass ecosystem — results from a ^{3}He/SF$_6$ tracer release experiment

Ryo Dobashi[1], David T. Ho[1]

[1]Department of Oceanography, University of Hawai'i at Mānoa, 1000 Pope Road, Honolulu, Hawaii 96822, USA

Correspondence to: Ryo Dobashi (rdobashi@hawaii.edu)

Abstract. Seagrass meadows are one of the most productive ecosystems in the world and could ~~play a role in~~help ~~mitigat~~eing the increase of atmospheric CO_2 from human activities. However, ~~U~~understanding ~~their~~ the role of seagrasses in the global carbon cycle requires knowledge of air-sea CO_2 fluxes and hence knowledge of the gas transfer velocity. In this study, gas transfer velocit~~y~~ies ~~and its controlling processes were examined in a seagrass ecosystem in south Florida. Gas transfer velocity was~~ were determined using the ^{3}He and SF$_6$ dual tracer technique in a seagrass ecosystem in south Florida, Florida Bay, near Bob Allen Keys (25.02663°N, 80.68137°W) between 1 and 8 April 2015. The observed gas transfer velocity normalized for CO_2 in freshwater at 20° C, $k(600)$, was 4.8 ± 1.8 cm h^{-1}, which was . ~~The resulting gas transfer velocities were~~ lower than ~~previous experiments in the coastal and open oceans at the same wind speeds. Therefore, using published~~ that calculated from published wind speed/gas exchange parameterizations ~~would overpredict gas transfer velocities and CO_2 fluxes in this area~~. The deviation in $k(600)$ from other coastal and offshore regions was only weakly correlated with tidal motion and air-sea temperature difference, implying that wind ~~must therefore still be~~is the dominant factor driving gas exchange. The lower gas transfer velocity was most likely due to wave attenuation by seagrass and limited wind fetch in ~~this~~ the study area. A new wind speed/gas exchange parameterization is proposed ($k(600) = 0.143u_{10}^2$), which might be applicable to other seagrass ecosystems and wind fetch limited environments.

1 Introduction

Seagrass meadows are one of the most productive ecosystems in the world and stock as much as 4.2–8.4 PgC in their soils (Fourqurean et al., 2012). Because some of the ~~the~~ organic carbon produced ~~via photosynthesis~~by seagrasses are refractory and accumulate ~~easily sinks to the bottom~~ on the seafloor ~~and some of the organic carbon stays in the ocean as a refractory matter~~, seagrass meadows are expected to be blue carbon sinks that ~~can~~ help mitigate the increase of anthropogenic CO_2. Seagrasses are estimated to bury 45−190 g C m^{-2} yr^{-1}, a significantly higher rate compared to terrestrial forests (0.7−13.1 g C m^{-2} yr^{-1}; Mcleod et al., 2011; Duarte et al., 2005). However, ~~R~~recently, the role of seagrasses in the global carbon cycle has been revisited, as ~~CO$_2$~~carbon emissions from seagrasses ~~CaCO$_3$ production~~ were found to be large (Howard et al., 2017; Van

30 dam et al., 2021; Schorn et al., 2021). Howard et al. (2017) examined the stock of organic and inorganic carbon in the soil of seagrass meadows in Florida Bay and southeastern Brazil, and found that the soils in both regions have more inorganic ~~carbon~~ than organic carbon;. ~~t~~They suggested that both regions ~~and~~ are sources of CO_2 to the atmosphere by assuming 0.6 mol of CO_2 is produced when 1 mol of $CaCO_3$ is produced. Schorn et al. (2021) ~~also~~ reported that the seagrasses in the Mediterranean Sea emit 106 μmol m^{-2} d^{-1} methane, mainly from their leaves.

35 Knowledge of the gas transfer velocity (k) is needed to understand the role of seagrass ecosystems in the global carbon cycle, since air-sea CO_2 flux is a function of k and the air-sea difference in the partial pressure of CO_2 (pCO_2). There are several methods to determine k in the field. The ^{3}He/SF$_6$ dual tracer technique, which we employed in this study, is a mass balance technique that involves injecting these tracers into the ocean and determining k by measuring the change in the ratio of the two gases with time. The direct flux techniques, such as ~~the~~ eddy covariance ~~method~~, measure the CO_2 flux in the air and CO_2
40 concentration both in the sea and air to derive k (McGillis et al. 2001). The k ~~can~~ has also be~~en~~ estimated from the heat ~~-~~transfer velocity ~~of heat~~ by assuming that the gas and heat transfer velocities are related by their diffusivities;. ~~however~~However, the estimated gas transfer velocity from heat, k_H, ~~have~~has been found to overestimate the actual k (e.g., Atmane et al., 2004).

Because k is difficult to measure, it is often parameterized using easily and widely measured parameters such as wind speed. In deep offshore regions, wind is known to predict the gas transfer velocity well since wind creates waves and currents,
45 which control turbulence and bubbles at the sea surface (Wanninkhof et al., 2009). Ho et al. (2018a) examined k in ~~the~~ Kaneohe Bay in Hawai'i and showed that k can be estimated well by wind speed where the depth is deeper than 10 m. On the other hand, in shallow regions, other parameters become important as well (e.g., Ho et al., 2016; 2018b). Ho et al. (2016) showed that k could be estimated well by wind speed and current speed in a shallow tidal estuary in south Florida, because the current enhances bottom-generated turbulence. Ho et al. (2018b) examined k in an emergent wetland where the depth < 1 m, and
50 showed that k can be parameterized ~~from~~by heat flux, rain rate, and current velocity ~~there~~. In the case of rain, rain rate is included in the parameterization because rainfall increases subsurface turbulence and k (Ho et al., 1997a, 2000).

In Florida Bay, k has been estimated from commonly used wind speed/gas exchange parameterizations. Zhang and Fischer (2014) determined the air-sea CO_2 flux to be 3.93 $\pm$ 0.91 mol m^{-2} yr^{-1} in Florida Bay; they used the wind speed/gas exchange parameterization determined from bomb-produced ^{14}C inventory in the ocean by Wanninkhof (1992). Van Dam
55 et al. (2020) estimated k by using heat as a proxy (k_H) in Florida Bay and found that k_H ~~wa~~is lower compared with k derived from published wind speed/gas exchange parameterizations when wind shear is relatively strong, even though k_H is known to overpredict k. This finding suggests that previous wind speed/gas exchange parameterizations are not ~~un~~suitable for the seagrass-dominated area and a specific parameterization for these fetch-limited environments is needed. In the study presented here, we use a ^{3}He/SF$_6$ tracer release experiment to determine k in a shallow seagrass-dominated environment to understand
60 processes that control k and to derive a parameterization for this environment.

2 Methods

2.1 Study site

65 ~~The ^{3}He/SF$_6$ tracer release experiments were~~was ~~conducted between 1 and 8 April 2015 near Bob Allen Keys~ in Florida Bay ~~(Fig. 1).~~ Florida Bay is ~~located in the southernmost part of Florida, USA. It is~~ situated between the Everglades marsh and the Florida Keys in the southernmost part of Florida, USA~~,~~ and covers approximately 2,000 km^2. In this bay, the average depth is less than 3.5 m, and the vertical extent of seagrasses is between 0.08 and 0.2 m (Sogard et al., 1989). *Thalassia testudinum* and *Laurencia* are the ~~dominate~~dominant seagrass and macroalgae, respectively, in the benthic communities, with an average standing crop of 63.6 and 8.9 g dry weight m^{-2}, respectively (Zieman et al., 1989). Seagrass density varies across

70 the bay, and its standing crop is 0−20 g dry weight m^{-2} in the summer around our study area (bottom figure in Fig. 1) (Zieman et al., 1989). The growth of seagrasses in Florida Bay ~~show~~ is seasonal~~ity~~, ~~and their~~with larger standing ~~crop~~crops ~~becomes larger~~ in spring and summer ~~and smaller~~than ~~in~~ in fall and winter (Zieman et al., 1999). The phytoplankton community is dominated by cyanobacteria, diatoms, and dinoflagellates (Philips and Badylak, 1996)~~,~~. with ~~frequent~~ ~~C~~cyanobacteria blooms ~~occur frequently~~ in the central north region of the bay due to nutrient input from the land (Philips et al., 1999; Lavrentyev et

75 al., 1998). Wind is persistent~~ly blows~~ from southeast to northwest during summer and from north to south during winter (Wang et al., 1994). ~~Current~~The current speed is about 0.02−0.14 m s^{-1} (Wang, 1998), and the tidal amplitude is 0.1−0.4 m (Wang et al., 1994). The ^{3}He/SF$_6$ tracer release experiments were conducted between 1 and 8 April 2015 near Bob Allen Keys (Fig. 1).

2.2 Tracer injection and ~~underway SF$_6$ measurement~~measurement

80 We injected ^{3}He and SF$_6$ at a ratio of 1:340 into the water at the study location (25.0107°N, 80.692°W; black cross~~green star~~ in Fig. 1) on 1 April 2015 for 1 minute via a length of diffuser tubing. After injection, we ~~performed underway SF$_6$ measurements using~~used an underway SF$_6$ analysis system (Ho et al., 2002) ~~that~~to measure~~d~~ surface water SF$_6$ concentrations ~~in the surface water~~ every ~45 s. The system is composed of a gas extraction unit, which continuously removes SF$_6$ from the water for measurement using a membrane contactor, and an analytical unit. ~~The gas extraction unit continuously removes

85 SF$_6$ from the water for measurement using a membrane contactor. The other unit is~~ composed of a gas chromatograph equipped with an electron capture detector (GC/ECD). ~~Based on previous experiments, t~~The system has a detection limit of 1×10^{-14} mol L^{-1} and an analytical precision of ±1% (Ho et al., 2018a). A personal computer showed the SF$_6$ concentration ~~displayed the SF$_6$ concentrations~~ in real time, which~~. This~~ ~~provided a spatial distribution of the SF$_6$ patch, which~~ guided the boat navigation and spatial survey.

90 ~~Around~~ Near the center of the SF$_6$ patch ~~between,~~ 1 and 8 April 2015, we conducted 26 total stations for depth profiles measurements of temperature and salinity with a conductivity, temperature, and depth (CTD) sonde and we took discrete ^{3}He and SF$_6$ sampl~~es at a subset of these stations~~ ~~April 1 and 8 2015 (green~~yellow triangles in Fig. 1). ~~ing (see~~ ~~next paragraph~~below).

In total, ~~2.3 Discrete ^{3}He and SF$_6$ measurements:~~

~~W~~we collected 16 ^{3}He samples (~40 mL each) and 84 discrete SF$_6$ samples. ^{3}He samples were taken ~~at 26 stations~~ in copper tubes mounted in aluminum channels and sealed at the ends with stainless steel clamps. ~~between~~ April 1 and 8 2015 (green triangles in Fig. 1). In the shore-based laboratory at the end of the experiment, ^{3}He and other gases were extracted from the water in the copper tubes ~~and~~. transferred to flame-sealed glass ampoules, and . ~~We measured~~ ^{3}He ~~concentration~~ measured

100
using a He isotope mass spectrometer (Ludin et al., 1998). 84 discrete SF$_6$ samples were taken at the same stations ~~(yellow triangles in Fig. 1)~~ using 50-mL glass syringes and submerged in water in a cooler until measurement back on shore at the end of each day. SF$_6$ was extracted by a headspace technique and measured on a GC/ECD as described by Wanninkhof et al. (1987). We used the mean ^{3}He and SF$_6$ concentration for each day to determine k, so there are six ^{3}He/SF$_6$ data points between 3 and 8 April ~~3 and 8~~ (Fig. 2f).

105

2.~~3~~4 Measurements of ~~wind, temperature, salinity and tide~~environmental variables

We measured wind speed, wind direction, and air temperature at ~5 m above sea level every 10 s using a sonic anemometer (Vaisala WMT700) near Bob Allen Keys (25.02663°N, 80.68137°W; blue dot in Fig. 1). The air temperature was averaged every 1 h to calculate the air-sea temperature difference (sea ~~temperature~~ minus air ~~temperature~~). ~~Additional wind speeds~~

110
~~measured using a sonic anemometer (Vaisala WXT532) at ~3 m above the sea level at 25.07209°N, 80.73511°W (pink square in Fig. 1, 7.4 km away from the blue dot) between 2015 and 2019 were obtained from~~ U.S. National Park Service (NPS) (https://www.ndbc.noaa.gov/) ~~Everglades National Park to compare k derived from this study and k estimated from published parameterizations.~~

~~Wind speed data were extrapolated to 10 m above the sea level using the~~ following ~~equation below (Amorocho and DeVries,~~

115
~~1980):~~

$$u_z = u_{10}\left(1 - C_{10}^{\frac{1}{2}}\kappa_c^{-1}\ln\left(10/z\right)\right) \text{~~———————————————~~} \tag{1}$$

~~where u_z is the wind speed at height z, κ_c is the von Kármán constant (0.41), C_{10} is the surface drag coefficient of wind at 10 m height (1.3×10^{-3}) (Stauffer, 1980).~~

Hourly tidal amplitude, ~~water~~ sea surface temperature, and salinity data from the same site (blue dot in Fig. 1) between

120
2015 and 2019 were obtained from NPS~~Everglades National Park~~ (https://www.ndbc.noaa.gov/). The tidal amplitude was measured using a digital shaft encoder (WaterLog H331), and sea surface. ~~Water~~ temperature and salinity were measured using multiparameter sondes (Hydrolab Quanta until 5 March 2019; OTT-Hydromet OTT-PLS-C thereafter). Additional wind speeds measured using a sonic anemometer (Vaisala WXT532) at ~3 m above the sea level at 25.07209°N, 80.73511°W (pink square in Fig. 1, 7.4 km away from the blue dot) between 2015 and 2019 were obtained from NPS to compare k derived from this

125
study and k estimated from published parameterizations.

Wind speed data were extrapolated to 10 m above the sea level using the equation below (Amorocho and DeVries, 1980):

$$u_z = u_{10}\left(1 - C_{10}^{\frac{1}{2}}\kappa_c^{-1}\ln(10/z)\right) \hspace{5cm} (1)$$

where u_z is the wind speed at height z, κ_c is the von Kármán constant (0.41), C_{10} is the surface drag coefficient of wind at 10 m height (1.3×10^{-3}) (Stauffer, 1980).

130   2.5. Underway pCO$_2$ Measurements

We measured the pCO$_2$ along the boat track (red linedots in Fig. 1) using an underway system based on the design of Ho et al. (1997b) and incorporating the suggestions from Pierrot et al. (2009). Water was pumped through a thermosalinograph (TSG) into a showerhead equilibrator, and a high precisionhigh-precision thermistor measured the temperature. The gas was dried by Nafion and $Mg(ClO_4)_2$ dryers, and was continuously circulated through a non-dispersive infrared (NDIR; LI-COR

135   LI-840A) analyzer. We stopped the flow during measurement and vented the NDIR cell to the atmosphere. The interval between measurements was 41 s. Atmospheric air was taken from an inlet at the bow of the boat through a length of aluminum/plastic composite tubing (Dekabon), and was diverted into the NDIR analyzer at specific times (every ~72 min). We calibrated the analyzer at regular time intervals (~72 min) with a 511 ppm CO_2 standard calibrated with a primary standard from NOAA/ESRL/GMD and a CO_2-free reference gas (UHP N_2 passed through soda lime to remove CO_2). In total, 1,261

140   and 13 xCO_2 data were taken from the water and air, respectively. With measured mole fraction of CO_2 (xCO_2), barometric pressure (P), and water vapor pressure at water surface temperature (Vp), we calculated the water and atmospheric pCO$_2$ by applying the following expression (DOE, 1994): pCO$_2$ = (P−Vp) × xCO_2. pCO$_2$ values were corrected for temperature shifts in the sample from the intake point (i.e., as measured by the TSG) to the pCO$_2$ system using an empirical equation proposed by Takahashi et al. (1993). Fugacity of CO_2 (fCO_2) was calculated by $fCO_2 = \alpha \times pCO_2$, where α is an activity coefficient

145   calculated from a formula in Wanninkhof and Thoning (1993). Additional fCO_2 data were obtained from National Oceanic and Atmospheric Administration (NOAA) Pacific Marine Environmental Laboratory (https://www.pmel.noaa.gov/) at 24.90°N, 80.62°W (cyan diamond in Fig. 1, 15 km away from the blue dot). CO_2 flux between air and water was calculated with solubility (K_0) and fCO_2 using the equation below:

$$F = kK_0(fCO_{2water} - fCO_{2air}), \hspace{5cm} (2)$$

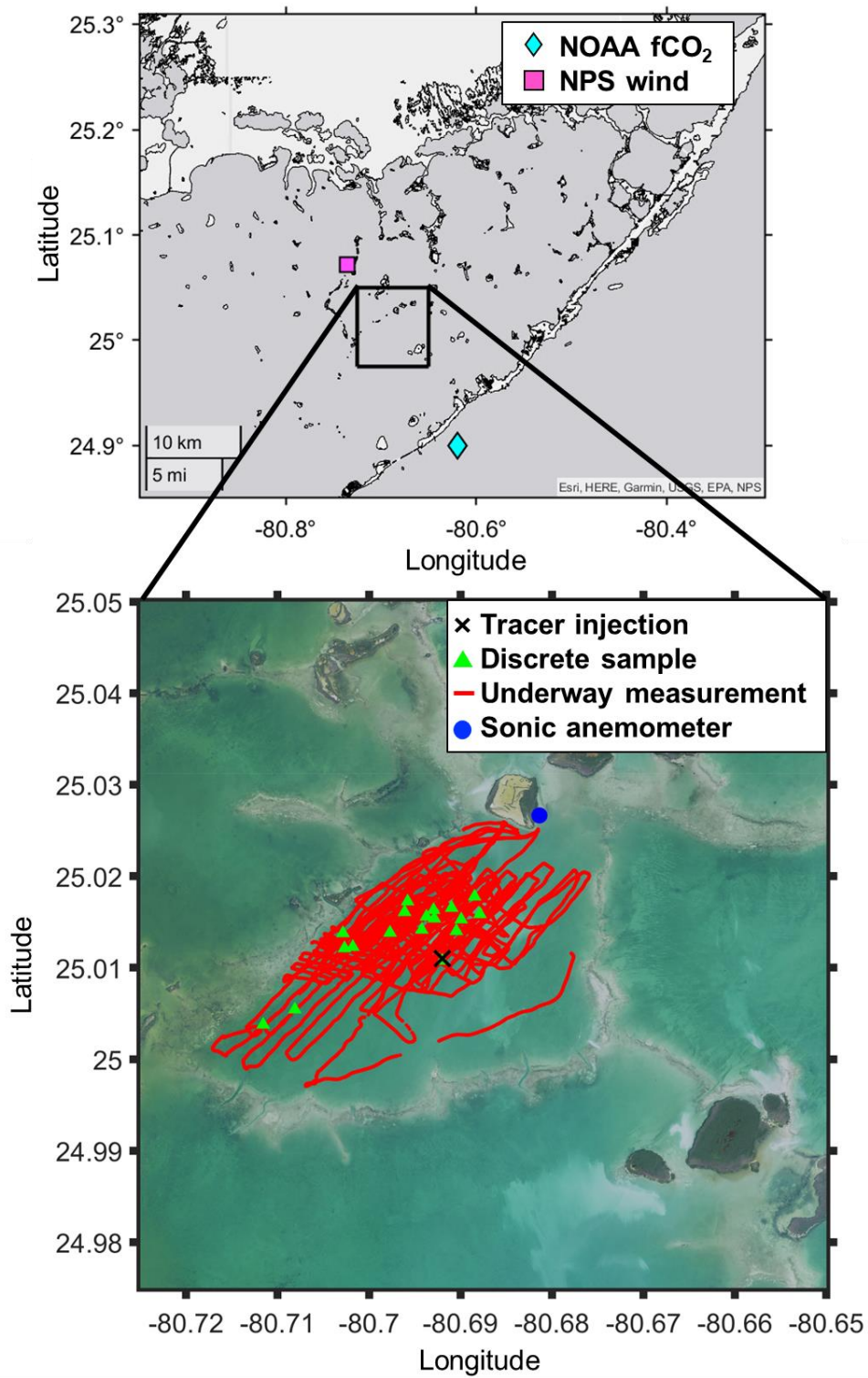150   where the K_0 was calculated from the measured temperature and salinity (Weiss, 1974).

Fig. 1 Map of the study area. ~~Green star~~The black cross is the ^{3}He and SF_6 injection location; red lines~~dots~~ are the boat track where underway measurement was conducted for pCO_2 and SF_6; the blue dot is the location where wind velocity, air temperature, water temperature, salinity, and tidal amplitude were measured; the green~~yellow~~ triangle is~~are~~ the stations where discrete samples for ^{3}He and SF_6 were taken; the pink square is where additional wind velocity was measured; and cyan~~aqua~~ diamond indicates where additional fCO_2 were measured. Note that water temperature, salinity, tidal amplitude, and additional wind velocity were obtained from ~~E NPS~~verglades National Park, and additional fCO_2 data were obtained from NOAA Pacific Marine Environmental Laboratory. Map data are generated by MATLAB geobasemap "darkwater" and downloaded from the Fish and Wildlife Research Institute (https://myfwc.com/research/) and NOAA Office for Coastal Management (https://www.noaa.gov/)

2.4~~6~~. Gas transfer velocity calculation~~measurement~~ and ^{3}He/SF_6 ratio modeling

The ~~two tracers, ^{3}He and SF_6, were injected together into the mixed layer at a constant ratio, and the ratio of ^{3}He/SF_6 was measured over time as described above. The~~ technique relies on the well-tested assumption that patch dilution, such as by horizontal mixing, affects the individual tracer concentrations but does not alter the ^{3}He/SF_6 ratio; the only process that changes the ^{3}He/SF_6 ratio is air-sea gas exchange. The gas transfer velocity for ^{3}He, $k\,_{^3\text{He}}$, can be determined as follows (Wanninkhof et al., 1993):

$$k\,_{^3\text{He}} = -\left(1 - \left(Sc_{SF_6}/Sc\,_{^3\text{He}}\right)^{-1/2}\right)^{-1} h\frac{\mathrm{d}}{\mathrm{dt}}\left(\ln\left(\,^3\text{He}_{exc}/SF_6\right)\right) \tag{3}$$

where Sc_{SF_6} and $Sc\,_{^3\text{He}}$ are the Schmidt numbers (i.e., the kinematic viscosity of water divided by diffusion coefficient of the gas in water) for SF_6 and ^{3}He, respectively (see section 2.5~~7~~). h is the measured water depth in Florida Bay, adjusted for tidal variation. ^{3}He$_{exc}$ is the ^{3}He in excess of solubility equilibrium with the atmosphere (used interchangeably with ^{3}He here). The gas transfer velocity measured during this experiment is normalized to $k(600)$, where 600 corresponds to Sc number of CO_2 in freshwater at 20°C:

$$k(600) = k\,_{^3\text{He}}\left(600/Sc\,_{^3\text{He}}\right)^{-1/2}. \tag{4}$$

~~2.7 Calculation of *Sc* number~~

~~In the literature, *Sc* is often calculated from a compilation by Wanninkhof (2014). However, because the salinity in Florida Bay is 40, which is higher than the range provided by Wanninkhof (2014), we have re-calculated *Sc* for an extended range here. In our calculation, the kinematic viscosity for fresh water and seawater are derived using equations given by Sharqawy et al. (2010). Molecular diffusion coefficients of various gasses for freshwater were calculated using empirical equations derived from previous studies (Jähne et al., 1987; Wilke and Chang, 1955; Hayduk and Laudie, 1974; King and Saltzman, 1995; Saltzman et al., 1993; Zheng et al., 1998; De Bruyn and Saltzman, 1997). While the effect of temperature on molecular diffusion coefficient is well investigated, the effect of salinity has been the subject of fewer studies. SF₆, methyl bromide (CH₃Br), and trichlorofluoromethane (CFC-11) do not have significant differences in diffusion coefficients between fresh~~

~~water and a 35 g L^{-1} sodium chloride (NaCl) solution (King and Saltzman, 1995; De Bruyn and Saltzman, 1997; Zheng et al.,~~
~~1998). However, diffusion coefficients for methane (CH~~$_4$~~), dichlorodifluoromethane (CFC-12), and He in seawater are 4–7%~~
~~less than the coefficients in freshwater (Jähne et al., 1987; Saltzman et al., 1993; Zheng et al., 1998). To represent the~~
~~dependence of molecular diffusion coefficients on salinity for gasses except for SF~~$_6$~~, CH~~$_3$~~Br and CFC-11, we linearly~~
~~inter/extrapolated the molecular diffusion coefficients for various salinities by assuming that the diffusion coefficients decrease~~
~~by 6% when the salinity is 35, compared with freshwater (Jähne et al., 1987; Wanninkhof, 2014). Molecular diffusion~~
~~coefficients for a salinity of 40 are about 7% smaller compared to the coefficients for freshwater based on this assumption.~~
~~Least squares fourth order polynomial fit, including the effect of salinity, was produced to predict the *Sc* numbers at various~~
~~temperatures and salinities (Table 1).~~

~~2.8 Modeling the decrease of ^{3}He/SF~~$_6$~~ ratio~~

The decrease of the ^{3}He/SF$_6$~~tracer~~ ratio was compared to the decrease predicted by published wind speed/gas exchange
parameterizations to assess the validity of these parameterizations for the study area. Under the assumption that air-sea gas
exchange is the only process that alters the ^{3}He/SF$_6$ ratio in the water, the change in ^{3}He/SF$_6$ ratio during this experiment can
be modeled by an analytical solution to equation (3):

$$\left(\, ^3He/SF_6 \right)_t = \left(\, ^3He/SF_6 \right)_{t-1} \exp\left(-\frac{k\,_{^3He}\Delta t}{h}\left(1 - \left(Sc_{SF_6}/Sc\,_{^3He} \right)^{-1/2} \right) \right) \tag{5}$$

where $(^3He/SF_6)_t$ is the ^{3}He to SF$_6$ ratio at time t and $(^3He/SF_6)_{t-1}$ is the ratio at the previous time step. $k\,_{^3He}$ is ~~predicted~~
determined from wind speeds measured during ~~this~~ the experiment and ~~existing~~ published parameterizations. The skill of the~~se~~
parameterizations to predict the measured ^{3}He/SF$_6$ during this experiment is evaluated in terms of the coefficient of variation
of the root mean square error (cvRMSE):

$$cvRMSE = \frac{\sqrt{\frac{1}{N}\sum_{n=1}^{N}\left(R_{mod}^n - R_{obs}^n \right)^2}}{\overline{R_{obs}}}, \tag{6}$$

where R_{obs}^n and R_{mod}^n are the observed and modeled ^{3}He/SF$_6$ tracer ratios, respectively, and N is the number of stations
sampled after the initial sampling (5 for table 2 and 2 for Fig. 5e). The ability of commonly used parameterizations, including
the quadratic relationships of Wanninkhof (1992), Nightingale et al. (2000), and Ho et al. (2006), the exponential relationship
of Raymond and Cole (2001), and the hybrid parameterization of Wanninkhof et al. (2009) to predict k in Florida Bay was
evaluated by examining the cvRMSE. Equation (6) was also used to derive the optimal coefficients (A) for a quadratic
($k = Au_{10m}^2$) parameterization by minimizing the cvRMSE. We regarded A with minimum cvRMSE as the best coefficient for
parameterization.

2.5 Calculation of *Sc* number

In the literature, *Sc* is often calculated from a compilation by Wanninkhof (2014). However, because the salinity in Florida
Bay ~~is 40, which is~~was higher than the range provided by Wanninkhof (2014)~~,~~ we ~~have~~ re-calculated *Sc* for an extended

215 salinity range here. In our calculation, tThe kinematic viscositiesy for fresh-water and seawater arewere deriveddetermined using equations given by Sharqawy et al. (2010), and the .mMolecular diffusion coefficients of various gasses for freshwater were calculated using empirical equations derived from previous studies (Jähne et al., 1987; Wilke and Chang, 1955; Hayduk and Laudie, 1974; King and Saltzman, 1995; Saltzman et al., 1993; Zheng et al., 1998; De Bruyn and Saltzman, 1997). While the effect of temperature on molecular diffusion coefficient is well investigatedstudied, the effect of salinity has been the

220 subject of fewer studies investigations. For SF$_6$, CH$_3$Br, and CFC-11, the diffusion coefficients in seawater are similar to those in freshwater (King and Saltzman, 1995; De Bruyn and Saltzman, 1997; Zheng et al., 1998). SF$_6$, methyl bromide (CH$_3$Br), and trichlorofluoromethane (CFC-11) do not have significant differences in diffusion coefficients between fresh-water and a 35 g L^{-1} sodium chloride (NaCl) solution (King and Saltzman, 1995; De Bruyn and Saltzman, 1997; Zheng et al., 1998). However, the diffusion coefficients for methane (CH$_4$), CFC-12, and He in seawater are 4-7% lower than those in freshwater

225 (Jähne et al., 1987; Saltzman et al., 1993; Zheng et al., 1998). To represent the dependence of molecular diffusion coefficients on salinity for gases other than SF$_6$, CH$_3$Br, and CFC-11, we linearly interpolated/extrapolated the molecular diffusion coefficients for different salinities by assuming that the diffusion coefficients decrease by 6% when the salinity is 35 compared to freshwater (Jähne et al., 1987; Wanninkhof, 2014). This assumption suggests that the diffusion coefficients for a salinity of 40 are approximately 7% smaller than those for freshwater. A least-squares fourth-order polynomial fit, incorporating the

230 effect of salinity, was used to predict Sc values at various temperatures and salinities However, diffusion coefficients for methane (CH$_4$), dichlorodifluoromethane (CFC-12), and He in seawater are 4-7% less than the coefficients in freshwater (Jähne et al., 1987; Saltzman et al., 1993; Zheng et al., 1998). To represent the dependence of molecular diffusion coefficients on salinity for gasses except for SF$_6$, CH$_3$Br and CFC-11, we linearly inter/extrapolated the molecular diffusion coefficients for various salinities by assuming that the diffusion coefficients decrease by 6% when the salinity is 35, compared with

235 freshwater (Jähne et al., 1987; Wanninkhof, 2014). Molecular diffusion coefficients for a salinity of 40 are about 7% smaller compared to the coefficients for freshwater based on this assumption. Least-squares fourth-order polynomial fit, including the effect of salinity, was produced to predict the *Sc* numbers at various temperatures and salinities (Table 1).

Table 1. Coefficients for a least-squares fourth-order polynomial fit of Schmidt number versus salinity and temperature for
240 various salinity and temperatures from 0 to 40°C.

Gas	A	a	B	b	C	c	D	d	E	e	Sc number (20°C, 0 PSU)	Sc number (20°C, 35 PSU)

^{3}He	334.38	0.90630	-17.566	-0.040902	0.53156	0.0011076	-0.0094081	1.8342×10^{-5}	7.1715×10^{-5}	1.3483×10^{-7}	132	146
He	377.10	1.1097	-19.810	-0.050665	0.59949	0.0013852	-0.010610	2.3081×10^{-5}	8.0880×10^{-5}	1.7028×10^{-7}	149	166
Ne	764.44	2.2495	-43.818	-0.11364	1.3943	0.0032933	-0.025331	5.652×10^{-5}	0.00019561	4.2289×10^{-7}	274	306
Ar	1876	5.5663	-131.69	-0.32458	4.9298	0.010744	-0.099518	0.00020223	0.00081784	1.5998×10^{-6}	549	619
O_2	1733.6	5.1437	-121.69	-0.29994	4.5556	0.0099283	-0.091963	0.00018688	0.00075576	1.4784×10^{-6}	507	572
N_2	2080.6	6.1735	-146.06	-0.35999	5.4677	0.011916	-0.11037	0.00022429	0.00090706	1.7743×10^{-6}	609	687
Kr	2036.2	5.9923	-133.13	-0.35181	4.5886	0.011183	-0.087051	0.00020169	0.00068746	1.5474×10^{-6}	623	695
Xe	2688.8	7.9128	-181.43	-0.48144	6.3779	0.015655	-0.12233	0.00028594	0.00091717	2.2082×10^{-6}	788	880
CH_4	1900.3	5.5923	-119.02	-0.31267	3.9947	0.009639	-0.074686	0.00017095	0.00058531	1.3002×10^{-6}	614	685
CO_2	1914.2	5.6330	-123.18	-0.32481	4.2040	0.010208	-0.079322	0.00018296	0.00062463	1.3992×10^{-6}	598	667
N_2O	2127	6.3112	-149.31	-0.36802	5.5897	0.012182	-0.11284	0.00022929	0.00092273	1.8139×10^{-6}	622	702

Gas	A	a	B	b	C	c	D	d	E	e	Sc (20, 0)	Sc (20, 35)
Rn	315.41	9.2820	-220.51	0.58779	7.9274	0.019612	-0.15397	0.00036344	0.00123 13	2.8283×10^-6	880	982
SF6	302.4	3.0926	-193.63	0.14258	6.5878	0.0035655	-0.12409	5.3058×10^-5	0.00097626	3.5673×10^-7	950	996
DMS	258.2.0	7.5983	-160.71	0.42182	5.3733	0.012946	-0.10025	0.00022905	0.00078480	1.7401×10^-6	841	938
CFC-12	346 0.3	10.183	-225.72	-0.5963	7.7688	0.018924	-0.14727	0.00034099	0.0011625	2.6148×10^-6	1061	1184
CFC-11	344 6.9	3.5251	-214.51	0.15589	7.1717	0.0037741	-0.1338	5.4896×10^-5	0.0010474	3.6378×10^-7	1123	1176
CH3Br	210.1	2.1487	-133.27	0.097717	4.5081	0.0024177	-0.084644	3.571×10^-5	0.00066483	2.3896×10^-7	668	700
CCl4	397 3.3	11.789	-278.92	0.68747	10.442	0.022756	-0.21078	0.00042832	0.0017322	3.3884×10^-6	1163	1312

$Sc = A + aS + (B+bS)T + (C+cS)T^2 + (D+dS)T^3 + (E+eS)T^4$ (T in °C). The last two columns are the calculated Schmidt number for 20°C, and salinities of 0 and 35 as examples, respectively. The diffusion coefficients, denominators of Sc, are derived from the following: ^{3}He, He, Ne, Kr, Xe, CH_4, CO_2 and Rn measured by Jähne et al. (1987); Ar, O_2, N_2, N_2O, and CCl_4 fit from Wilke and Chang (1955) adapted by Hayduk and Laudie (1974); SF_6 measured by King and Saltzman (1995); DMS measured by Saltzman et al. (1993); CFC-11 and CFC-12 measured by Zheng et al. (1998); CH_3Br measured by De Bruyn and Saltzman (1997). Sc numbers for temperature of 20°C and salinity of 35 become larger than Sc numbers for temperature of 20°C and salinity of 0 by 4.7–4.8% for SF_6, CFC-11 and CH_3Br and 10.8–12.8% for other gasses, respectively. Note that the fits are based on simple assumptions (see section 2.5), and the dependence of Sc on salinity needs to be investigated further in the future.

3. Results and discussion

3.1 Environmental parameters

During the experiment, wind ~~direction~~ was predominately from the east, and wind speeds increased towards the latter part of the study period (Fig. 2a). The mean and the standard deviation of the wind speed during the study period was 5.5 ± 2.0 m s^{-1} (range=0.12–12 m s^{-1}). ~~Mean w~~Water temperature showed a diurnal pattern with a mean and standard deviation of 26.3 ± 1.3°C (Fig. 2b). The diurnal pattern of the air temperature was weak, ~~as~~ with ~~athe~~ mean and standard deviation ~~were~~ of 25.1 ± 0.6°C. The air-sea temperature difference showed diurnal cycles, which ~~was~~were mainly driven by the diurnal cycle of the sea temperature, consistent with observations by Van Dam et al. (2020). Salinity ~~was~~ remained consistent throughout the study period (41 ± 0.1~~)~~; not shown). The tide consistently showed semidiurnal cycles with an amplitude of ≤ 0.2 m throughout the study period.

(a) Wind

wind speed (m/s)

(b) Air and water temperature

Temperature (°C)

air
water

(c) Air-water temperature difference (water − air)

Temperature (water − air; °C)

(d) Tide

Tidal amplitude (m)

(e) Gas transfer velocities

$k(600)$ (cm h^{-1})

(f) ^{3}He/SF$_6$

^{3}He/SF$_6$

1   2   3   4

Observations
This study: $k(600)=0.143\ u^2$
Wanninkhof (1992)
Nightingale et al. (2000)
Raymond and Cole (2001)
Ho et al. (2006)
Wanninkhof et al. (2009)

Apr 3   Apr 4   Apr 5   Apr 6   Apr 7   Apr 8
2015   (Local time)

13

Fig. 2 Time series of (a) hourly averaged wind vector at 10 m height (m s^{-1}), (b) water temperature and air temperature (°C), (c) temperature difference (water temperature minus air temperature; units: °C), (d) tidal amplitude (units: m) and (e) measured and estimated *k*(600) which is the gas transfer velocities normalized for 20°C freshwater CO_2 ~~at in situ temperature and salinity~~ and (f) measured and modeled change in ^{3}He/SF_6. Note that the wind direction is towards the north when the vector is towards the left. The time zone is local time. The figure legend for (e) is the same as that in (f). The numbers in (f) indicate the periods corresponding to the x-axis in Fig. 5.

3.2 Gas transfer velocity in Florida Bay and assessment of published parameterization

The measured *k*(600) was 4.8 ± 1.8 cm h^{-1} (mean ± s.d.) (Figs. 2e and 3), which was lower than previous studies conducted in coastal and open oceans at the same wind speed (Fig. 3 of Ho & Wanninkhof, 2016). A new parameterization was produced based on results from this experiment by minimizing the cvRMSE of $A \cdot u_{10}^2$, where A is a coefficient (Fig. 4):

$$k(600) = 0.143u_{10}^2 \tag{7}$$
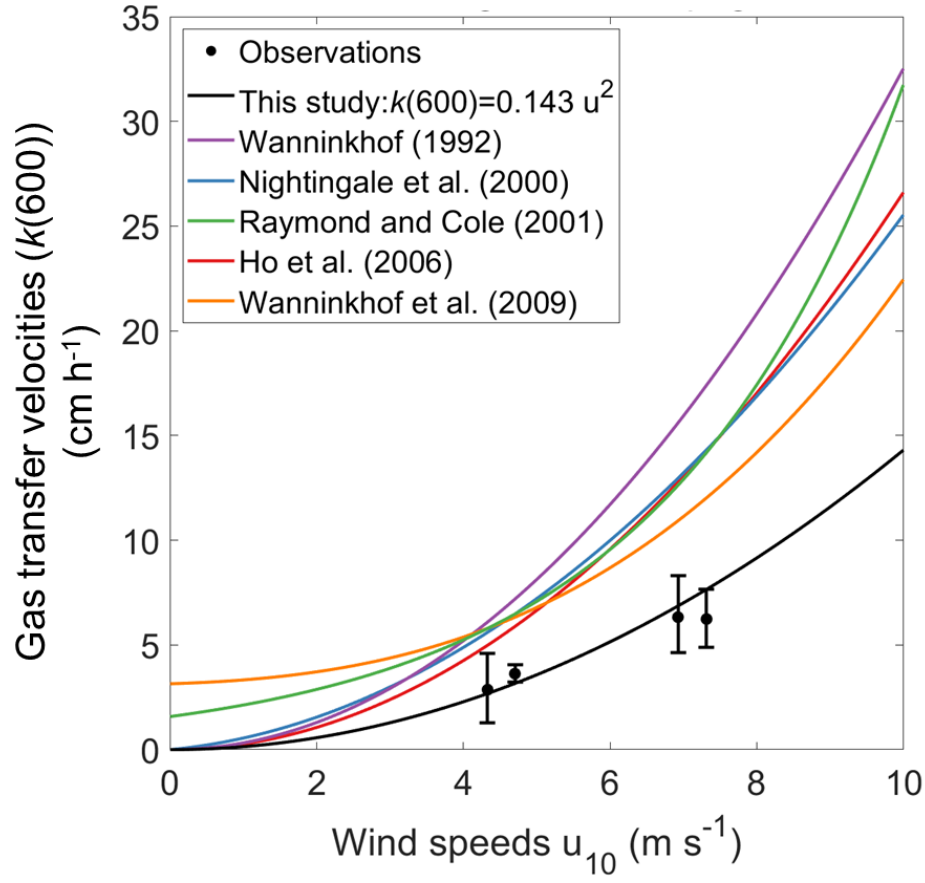
Fig. 3 Measured and modeled $k(600)$ (units: cm h^{-1}) with wind speed at 10 m height (units: m s^{-1}).
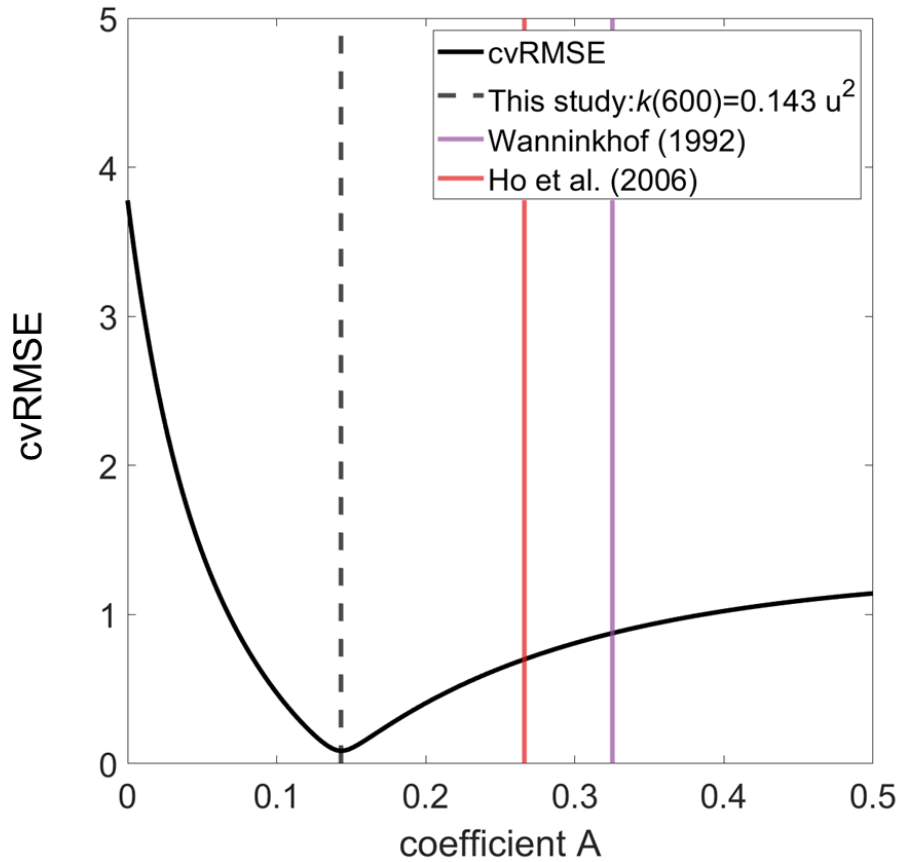
Fig. 4 The relationship between cvRMSE and the coefficient A in the equation $k(600)=A\ u_{10}^2$. Three vertical lines indicate the coefficients derived from this study, as well as those of Ho et al. (2006) and Wanninkhof (1992) from left to right. Note that $k(660)$ in Wanninkhof (1992) was converted to $k(600)$ by assuming that they scale as Sc to the power of $-1/2$.

The cvRMSE between the measured $^3He/SF_6$ and this new parameterization, equation (7), was 8.6%, while the cvRMSEs calculated from previously published wind speed/gas exchange parameterizations were more than 70% (Table 2). The coefficient of 0.143 was 46% and 56% lower than the $k(600)$ of 0.266 and 0.325 from Ho et al. (2006) and Wanninkhof (1992), respectively (Fig. 3). The result of previous studies ~~which~~ that used the parameterization of Wanninkhof (1992) in Florida Bay was modified in section 3.3~~2~~. The estimated k(600) ~~for CO₂ at in-situ temperature and salinity~~ derived from equation (7) was ~~6.3~~5.5±3.0~~3~~ cm h^{-1}, while all the published parameterizations estimated over 9.0~~10~~ cm h^{-1} on average between 3 and 8 April 2015 (Table 2 and Fig. 2e). k for CO_2 at in-situ temperature and salinity between 2015 and 2019 were also calculated using

16

~~the~~ equation (7) and the previously published parameterizations (Table 3). Annual averaged k ranged between 3.7–4.3 cm h^{-1} in Florida Bay between 2015 and 2019, while published parameterization would ~~yields~~yield values of 6.9–11.6 cm h^{-1}.

~~The deviations of between observed ^{3}He/SF$_6$ and modeled ^{3}He/SF$_6$, which is derived from published parameterizations, become larger with time, as shown in(Figure 2f). This means indicates that the published parameterizations overpredict k in~~
295 ~~Florida Bay, which is consistent with the result findings of Van Dam et al. (2020).~~

Table 2. Gas transfer velocities determined from <u>this study and </u>published parameterization.

References	Parameterization	Mean $k(600)$ (cm h^{-1})	cvRMSE
This study	$k(600)= 0.143u_{10}^2$	5.5±3.0	8.6%
Wanninkhof (1992)	$k(660)=0.31u_{10}^2$	12.4±6.8	87.5%
Nightingale et al. (2000)	$k(600)=0.333u_{10} + 0.222u_{10}^2$	10.4±5.2	76.0%
Raymond and Cole (2001)	$k(600)=1.58e^{0.3u_{10}}$	10.7±5.3	78.2%
Ho et al. (2006)	$k(600)=0.266u_{10}^2$	10.2±5.5	70.0%
Wanninkhof et al. (2009)	$k(660)=3+0.1u_{10} + 0.064u_{10}^2$ $+ 0.011u_{10}^3$	9.4±3.8	73.1%

The observed $k(600)$ was 4.8 ± 1.8 cm h^{-1} (average ± standard deviation). Note that $k(660)$ ~~is~~ <u>was </u>converted to $k(600)$ by assuming that the scale by Sc to the power of –1/2.

300

Table 3. Gas transfer velocities of CO_2 at in-situ temperature and salinity in Florida Bay between 2015 and 2019 <u>calculated</u>~~determined~~ using the wind speed/gas exchange parameterization determined here and ~~predicted using~~<u>from</u> published parameterizations.

Parameters		2015	2016	2017	2018	2019	Between 2015 and 2019
Wind speed (m s^{-1})		4.2±2.4	4.4±2.6	4.1±2.7	4.4±2.5	4.7±2.4	4.4±2.5 (range=0–27.5)
Sea temperature (°C)		27.6±3.8	26.7±4.1	26.8±3.9	26.7±4.2	27.3±3.8	27.0±4.0 (range=13.2–36.2)
Salinity		40.5±4.0	34.1±3.6	34.7±5.2	33.0±2.7	39.5±2.9	36.3±4.8 (range=24.5–51.8)
Tidal amplitude (m)		0.16±0.03	0.17±0.03	0.18±0.06	0.18±0.03	0.18±0.03	0.17±0.04 (range=0.04–0.33)
Mean k for CO$_2$ (cm h^{-1})	This study	3.7±4.0	4.0±4.1	3.8±5.6	4.0±4.1	4.3±4.4	3.6±4.2 (range=0–108)
	Wanninkhof (1992)	8.4±9.1	9.0±9.4	8.7±12.8	9.1±9.4	9.9±9.9	8.3±9.6 (range=0–247)
	Nightingale et al. (2000)	7.3±7.0	7.8±7.3	7.4±9.6	7.8±7.3	8.5±7.6	7.1±7.4 (range=0–176)
	Raymond and Cole (2001)	8.5±8.9	8.9±9.1	11.6±86.2	9.1±10.4	9.7±10.0	8.7±36 (range=1.6–6127)
	Ho et al. (2006)	6.9±7.4	7.4±7.7	7.1±10.4	7.4±7.7	8.1±8.1	6.8±7.9 (range=0–202)
	Wanninkhof et al. (2009)	7.8±5.4	8.1±5.5	8.2±10.1	8.1±5.7	8.6±6.0	7.4±6.4 (range=3.1–298)

The standard deviation of Raymond and Cole (2001) ~~were~~was large in 2017 since wind speed was as high as 27.5 m s^{-1}, and k was as high as 6.1×10^3 cm h^{-1}.

The deviations between observed and modeled ^{3}He/SF$_6$, which is derived from published parameterizations, become larger with time (Figure 2f). This indicates that the published parameterizations overpredict k in Florida Bay, which is consistent with the findings of Van Dam et al. (2020).

Van Dam et al. (2020) estimated ~~the air-sea gas transfer velocity~~k using heat as a proxy (k_H) in Florida Bay. They found that k_H was lower than k calculated from published parameterization even though k_H is known to overpredict k. They suggested that the stratification due to temperature restricts air-sea gas exchange since the deviation between k_H and k from commonly-used parameterization was large when the air-sea temperature difference was large. To investigate the relationship between environmental parameters and the deviation between measured and estimated air-sea gas exchange, we examined the relationship between temperature difference and the deviation between observation and the models by calculating cvRMSE separately in four periods (Fig. 5). We found no clear relationship between the deviation and air-sea temperature difference. The deviation observed in Van Dam et al. (2020) might be due to the fact that k_H contains the air-sea temperature difference in its equation (equation 7 in Van Dam et al. 2020); k_H becomes smaller when the air-sea temperature difference is large and vice versa. The deviation between observation and models was generally larger when wind speed was higher. cvRMSE became the largest values for all parameterizations in Period 4 when the mean wind speed was 7.3 m s^{-1}.

The new wind speed/gas exchange parameterization predicts the observed change in ^{3}He/SF$_6$ well (Fig. 2f and Table 2), suggesting that wind is the dominant factor controlling gas exchange in this area. In Florida bay, waves are damped by seagrasses (Prager and Halley, 1999), which ~~might~~ could be one of the causes of lower k in this study. There is also the possibility that limited wind fetch in this region led to relatively weak waves and turbulence compared to other regions, contributing to lower k. Wind fetch is limited in this region~~,~~ since the wind mostly blows from east to west, and the Florida Keys restricts the water exchange between the bay and the Atlantic Ocean (Fig. 1 and Fig. 2a). There was almost no rainfall to affect k during the study period. T~~he t~~idal amplitude was small (~0.1 m) (Fig. 2d), suggesting that the bottom-generated turbulence was weak.
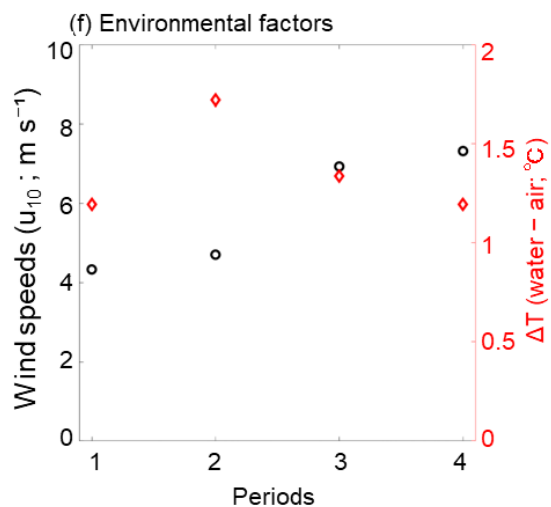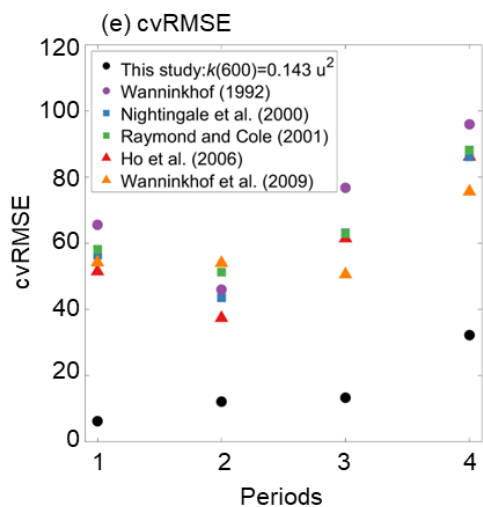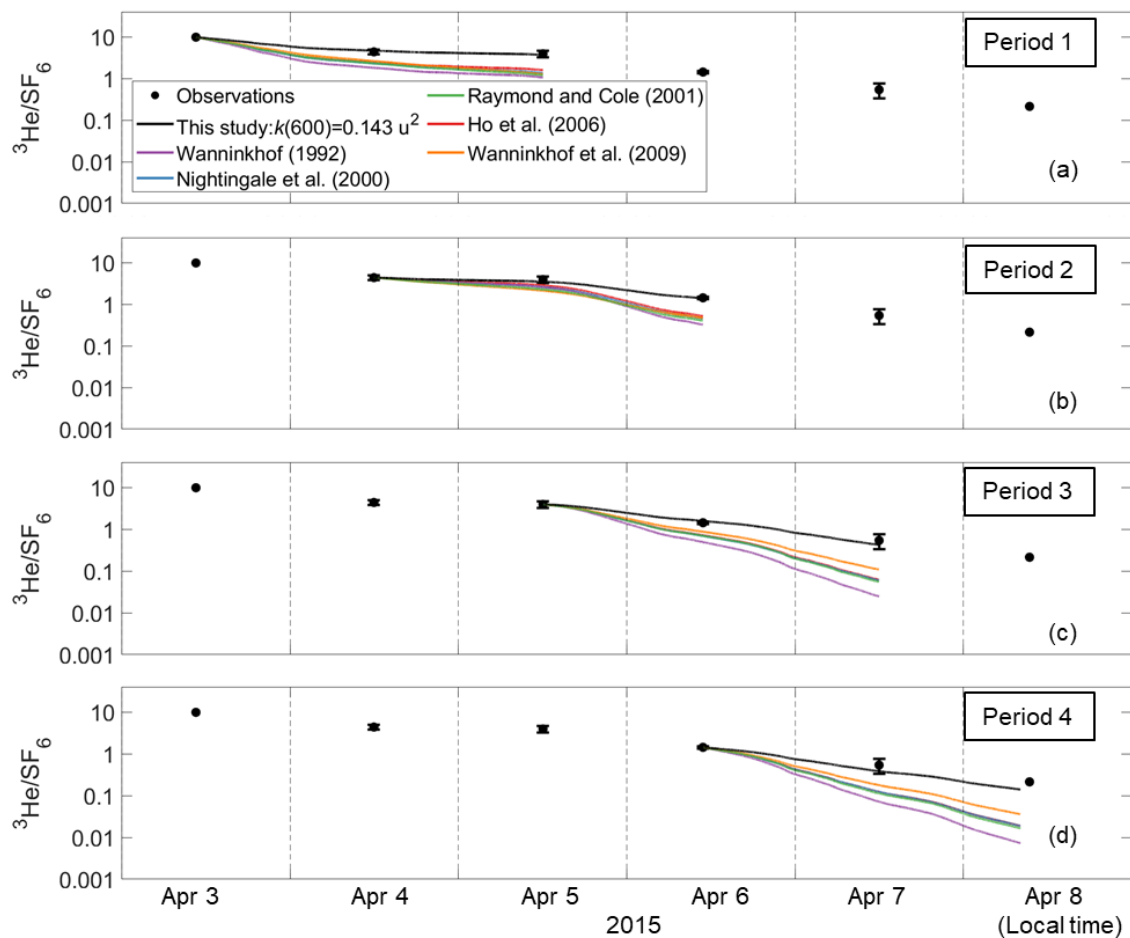
Fig. 5 Time series of measured and modeled change in ^{3}He/SF$_6$ in (a) period 1, (b) period 2, (c) period 3, and (d) period 4 in Fig. 2f. ^{3}He/SF$_6$ value is set to the starting point of each period. (e) The cvRMSE, (f) mean wind speed (m s^{-1}) and air-sea temperature difference (°C) during the period of 1–4. The x-axis represents the periods in Fig. 2f.

3.3~~2~~ Implications for biogeochemistry

Although the experiment was conducted over a short period of 8 days, our new parameterization, equation (7), fit the observations well; This implies that equation (7) can be applied even in different seasons and years if the wind speed is in the range of 0.12–12 m s^{-1} and seagrass conditions are similar (dominant seagrass of *Thalassia testudinum* has 63.6 (range=0–215) g dry weight m^{-2} standing crop in Florida Bay (Zieman et al., 1989)). The parameterization determined in this study should be applicable to other seagrass ecosystems as well~~,~~ since seagrass ecosystems are typically in coastal regions. In these environments, waves are damped by seagrasses and limited fetch. This wind speed/gas exchange parameterization proposed here might be applicable not only in seagrass ecosystems but also in other wind-fetch limited areas. To assess the applicability of this new parameterization in other inland ecosystems, additional ^{3}He/SF$_6$ dual tracer experiments will need to be conducted. Specifically, measuring the seagrass density and conducting dual-tracer experiments simultaneously is needed to relate the k and vegetation distribution.

The observed daytime pCO_{2water} and pCO_{2air} were 22~~48~~ ± 1~~26~~ and 39~~13~~ ± 3 µatm, respectively (Fig. 6a). The pCO_{2water} of 22~~48~~ ± 1~~26~~ µatm was in the range shown by Zhang and Fischer (2014), who examined the pCO_{2water} in the whole basin of the Florida Bay from 2006 to 2012, and showed that pCO_{2water} minim~~ua~~um was ~200 µatm in April (Fig. 3 of Zhang and Fischer 2014). Since the observed pCO_{2water} was lower than pCO_{2air}, CO_2 goes from the air to the sea during the daytime in the observation period (between 3 and 8 April 2015). The calculated daytime CO_2 flux using the measured pCO_2 difference and modeled k in this study (Black solid line in Fig. 2e) was −5.3 ± 3.0 mmol m^{-2} day^{-1} (negative value denotes CO_2 flux from the air to the water) (Fig. 6b). The CO_2 flux varied both within a day and between days mainly due to the variability in k (Note that k(600) in Fig. 2e is filtered with 25 minutes running average). Diurnal fCO$_{2water}$ amplitude at the NOAA station (cyan diamond in Fig. 1) between 3 and 8 April 2015 was as small as 25–53 µatm, and so we calculated daily CO_2 flux by assuming CO_2 difference between air and water during the night is the mean daytime CO_2 difference. The calculated daily CO_2 flux ~~using the measured pCO_2 difference and modeled k in this study (Black solid line in Fig. 2e)~~ was −7.0~~4.4~~ ± 3.5~~2.6~~ mmol m^{-2} day^{-1} ~~(negative value means CO_2 goes from the air to the sea) (Fig. 6b).~~, which was~~ ~~ higher than daytime CO_2 flux because wind speed was higher during the night. ~~Although we did not conduct pCO_2 measurement during the night and so the calculated value is biased toward daytime, the daily averaged pCO_{2water} and CO_2 flux during the whole observation period would still be lower than pCO_{2air} and negative, respectively, considering that the observed pCO_2 was as low as 228 µatm and the CO_2 flux at the NOAA station (aqua diamond in Fig. 1) was always negative with diurnal fCO$_{2water}$ amplitude of 25-53 µatm between April 3 and 8, 2015.~~

21

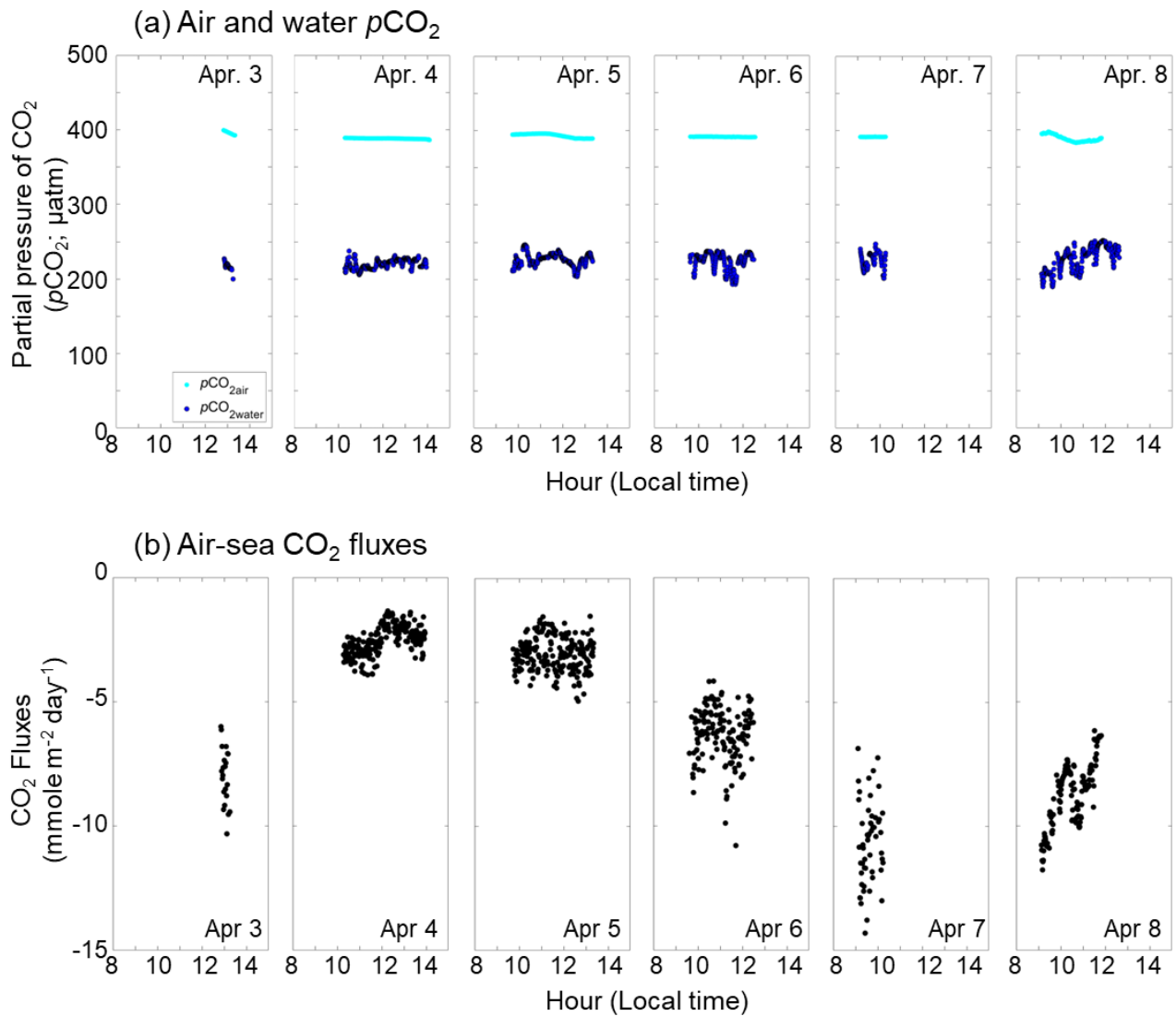**Fig. 6** Time series of (a) measured pCO_{2water} (blue dots) and pCO_{2air} (cyan dots) (units: μatm), (b) calculated CO_2 flux (units: mmole m^{-2} day^{-1}). Negative CO_2 flux indicates that the sea is a sink of CO_2. The time zone is local time.

370   Contrary to our experimental period, the aAnnual averaged CO_2 flux is, however, known to be from the water to the air in Florida Bay (e.g., Zhang and Fischer, 2014; Van dam et al., 2021). The pCO_2 and CO_2 flux in Florida Bay are suggested to have seasonality due to cyanobacteria blooms (Zhang and Fischer, 2014). The seasonality of seagrasses may also contribute to the seasonality of pCO_2 and CO_2 flux, as its productivity also shows seasonality (higher in spring and summer and lower in fall and winter) (Zieman et al., 1999). Zhang and Fischer (2014) measured the pCO_{2water} for the whole area of the Florida Bay

375   and estimated the CO_2 flux in Florida Bay to be 3.93 ± 0.91 mol m^{-2} yr^{-1} using the parameterization of Wanninkhof (1992);

22

we recalculated the CO_2 flux to be 1.73 ± 0.40 mol m^{-2} yr^{-1} by multiplying 0.44 (e.g., 1 minus 0.56; see section 3.2). By conducting atmospheric eddy covariance measurements near the Bob Allen Keys (blue dot in Fig. 1), Van Dam et al. (2021) showed that the CO_2 flux in Florida Bay was~~is~~ 6.1–7.0 mol m^{-2} year^{-1}, which is significantly higher than the corrected value of 1.73 ± 0.40 mol m^{-2} yr^{-1} ~~in Zhang and Fischer (2014)~~. Although the reason is not clear, primary production by phytoplankton and seagrasses might be lower when Van Dam et al. (2021) conducted their observation (2019–2020), resulting in higher CO_2 flux from sea to air, since there is no negative mean CO_2 flux in spring when they conducted their measurements (Fig. 1a in Van Dam et al., 2021). Van Dam et al. (2021) also calculated the excess CO_2, which is the CO_2 concentration difference between water and air to achieve the annual CO_2 flux of 6.1–7.0 mol m^{-2} year^{-1}, in Florida Bay to be between 5.2 and 6.0 µmol kg^{-1}, using a mean k of 11.7 cm h^{-1}; we recalculated the excess CO_2 to be between 14 and 16 µmol kg^{-1} using the k of 4.3 cm h^{-1} ~~, which is~~ parameterized from th~~is~~e current study (Table 3). The recalculated excess CO_2 almost double~~s~~ the~~ir~~ calculation of Van Dam et al. (2021) ~~5.2–6.0 µmol kg^{-1}~~ and ~~hence~~ requires significantly more CO_2 input.

4. Summary

Air-sea gas exchange was investigated in a seagrass ecosystem in South Florida, USA, using the ^{3}He and SF_6 dual tracer technique. The gas transfer velocity was lower than that in other coastal areas and open oceans, and commonly-used wind speed/gas exchange parameterizations ~~tend to~~ overpredict the gas transfer velociti~~es~~y, especially when wind speeds were~~as~~ relatively high (> 7 m s^{-1})~~strong~~. A new wind speed/gas exchange parameterization was proposed ($k(600) = 0.143u_{10}^2$), which was able to predict ~~fitted well to~~ the observed gas~~—~~ transfer velocities significantly better than existing parameterizations~~exchange~~. This result suggests that wind is the dominant factor controlling gas exchange in the studied seagrass ecosystem, but the lower gas transfer velocity at a given wind speed was due to limited wind fetch in the study area and wave attenuation by seagrass. To assess the wider applicability of the proposed wind speed/gas exchange parameterization, more tracer release experiments are needed at similar inland ecosystems.

Author contributions

DH conceived, designed, and conducted the experiment. RD performed the data analysis.

Competing interests

The authors have declared that they have no competing interests.

Disclaimer

420 **Review statement**

References

Abril, G., Commarieu, M. V., Sottolichio, A., Bretel, P., and Guerin, F.: Turbidity limits gas exchange in a large macrotidal
425 estuary, Estuarine, Coastal and Shelf Science., 83(3), 342-348, 2009.

Amorocho, J., and DeVries, J. J.: A new evaluation of the wind stress coefficient over water surfaces,. Journal of Geophysical Research: Oceans., 85(C1), 433-442, 1980.

Atmane, M. A., Asher, W. E., and Jessup, A. T.: On the use of the active infrared technique to infer heat and gas transfer velocities at the air-water free surface,. Journal of Geophysical Research: Oceans., 109(C8), 2004.

430 De Bruyn, W. J., and Saltzman, E. S.: Diffusivity of methyl bromide in water,. Mar. Chem., 57:55-59,. doi:10. 1016/S0304-4203(96)00092-8, 1997.

DOE.: Handbook of Methods for the Analysis of the Various Parameters of the Carbon Dioxide System in Sea Water, Version 2, edited by A. G. Dickson and C. Goyet, ORNL/CDIAC-74, 1994.

Duarte, C. M., Middleburg, J. J., and Caraco, N.: Major role of marine vegetation on the oceanic carbon cycle, Biogeosciences 2: 1–8, 2005.

Fish and Wildlife Research Institute: https://www.fgdl.org/metadataexplorer/explorer.jsp, last access: 16 December 2022.

Fourqurean, J. W., and others.: Seagrass ecosystems as a globally significant carbon stock, Nat. Geosci., 5: 505–509, doi:10.1038/ngeo1477, 2012.

Ho, D. T., and Wanninkhof, R.: Air-sea gas exchange in the North Atlantic: 3He/SF6 experiment during GasEx-98, Tellus Series B., 68(1), 30198, https://doi.org/10.3402/tellusb.v68.30198, 2016.

Ho, D. T., Asher, W. E., Bliven, L. F., Schlosser, P., and Gordan, E. L.: On mechanisms of rain-induced air-water gas exchange, Journal of Geophysical Research: Oceans, 105(C10), 24045-24057, 2000.

Ho, D. T., Bliven, L. F., Wanninkhof, R. I. K., and Schlosser, P.: The effect of rain on air-water gas exchange, Tellus B., 49(2), 149-158, 1997a.

Ho, D. T., Ho, Wanninkhof, R., Masters, J., Feely, R. A., and Cosca, C. E.: Measurements of underway fCO_2 in the eastern equatorial Pacific on NOAA ships Malcolm Baldridge and Discoverer from February to September, 1994, Rep. ERL AOML-30, 52 pp., NTIS, Springfield, Va, 1997b.

Ho, D. T., Schlosser, P., and Caplow, T.: Determination of longitudinal dispersion coefficient and net advection in the tidal Hudson River with a large-scale, high resolution SF_6 tracer release experiment. Environmental Science & Technology, 36(15), 3234–3241, doi:10.1021/es015814+, 2002.

Ho, D. T., Law, C. S., Smith, M. J., Schlosser, P., Harvey, M., and Hill, P.: Measurements of air-sea gas exchange at high wind speeds in the Southern Ocean: Implications for global parameterizations, Geophys. Res. Lett., 33, L16611, doi:10.1029/2006GL026817, 2006.

Ho, D. T., Coffineau, N., Hickman, B., Chow, N., Koffman, T. and Schlosser, P.: Influence of current velocity and wind speed on air-water gas exchange in a mangrove estuary, Geophys. Res. Lett., doi:10.1002/2016GL068727, 2016.

Ho, D. T., De Carlo, E. H., and Schlosser, P.: Air-sea gas exchange and CO_2 fluxes in a tropical coral reef lagoon, J. Geophys. Res. Oceans., 123: 8701–8713, doi:10.1029/2018JC014423, 2018a.

Ho, D. T., Engel, V. C., Ferrón, S., Hickman, B., Choi, J., and Harvey, J. W.: On factors influencing air-water gas exchange in emergent wetlands. Journal of Geophysical Research: Biogeosciences, 123(1), 178–192, https://doi.org/10.1002/2017JG004299, 2018b.

Howard, J.L., Creed, J.C., Aguiar, M.V.P., Fourqurean, J.W.: CO_2 released by carbonate sediment production in some coastal areas may offset the benefits of seagrass "Blue Carbon" storage, Limnol Oceanogr., 63: 160–172, doi:https://doi.org/10.1002/lno.10621, 2017.

Hayduk, W., and Laudie, H.: Prediction of diffusion coefficients for nonelectrolytes in dilute aqueous solutions, AIChE Journal., 20(3), 611–615, https://doi.org/10.1002/aic.690200329, 1974.

Jähne, B., Munnich, K. O., Bosinger, R., Dutzi, A., Huber, W., and Libner, P.: On the parameters influencing air-water gas exchange, Journal of Geophysical Research., 92, 1937–1949, https://doi.org/10.1029/JC092iC02p01937, 1987.

King, D. B., and& Saltzman, E. S.: Measurement of the diffusion coefficient of sulfur hexafluoride in water,. Journal of Geophysical Research,. 100, 7083–7088,. https://doi.org/10.1029/94jc03313, 1995.

470 Lavrentyev, P. J., Bootsma, H. A., Johengen, T. H., Cavaletto, J. F., and& Gardner, W. S.: Microbial plankton response to resource limitation: insights from the community structure and seston stoichiometry in Florida Bay, USA,. Marine Ecology Progress Series,. 165: 45–57, 1998.

Ledwell, J. R.: The variation of the gas transfer coefficient with molecular diffusivity. In W. Brutsaert, & G. H. Jirka (Eds.), Gas transfer at water surfaces (pp. 293–302),. Hingham, MA: Reidel,,. https://doi.org/10.1007/978-94-017-1660-
475 4_27, 1984.

Ludin, A., Weppernig, R., Bönisch, G., & Schlosser, P.: Mass spectrometric Measurementmeasurement of helium isotopes and tritium in water samples, Technical Report Rep.. 98–6, 42 pp, Lamont-Doherty Earth Observatory, Palisades, NY, 1998.
McGillis, W. R., Edson, J. B., Hare, J. E., & Fairall, C. W.: Direct covariance air-sea CO2 fluxes, Journal of geophysical research: Oceans, 106(C8), 16729-16745, 2001.

480 Mcleod, E., Chmura, G. L., Bouillon, S., Salm, R., Björk, M., Duarte, C. M., ... and& Silliman, B. R.: A blueprint for blue carbon: toward an improved understanding of the role of vegetated coastal habitats in sequestering CO2,. Frontiers in Ecology and the Environment, 9(10), 552-560, 2011.

Nightingale, P. D., Malin, G., Law, C. S., Watson, A. J., Liss, P. S., Liddicoat, M. I., Boutin, J., and Upstill-Goddard, R. C.: In situ evaluation of air-sea gas exchange parameterizations using novel conservative and volatile tracers, Global Biogeochem.
485 Cycles,. 14, 373–387, doi:10.1029/1999GB900091, 2000.

NOAA National Data Buoy Center: https://www.ndbc.noaa.gov/station_page.php?station=bobf1, last access: 16 December 2022.

NOAA Office for Coastal Management: https://chs.coast.noaa.gov/htdata/raster2/imagery/FL_NAIP_2017_8754/, last access: 16 December 2022.

490 NOAA Pacific Marine Environmental Laboratory: https://www.pmel.noaa.gov/co2/story/Cheeca+Rocks, last access: 16 December 2022.

Philips, E. J., and Badylak, S.: Spatial variability in phytoplankton standing crop and composition in a shallow inner-shelf lagoon, Florida Bay, Florida, Bull. Mar. Sci., 58, 203–216, 1996.

Phlips, E. J., Badylak, S. and Lynch, T. C.: Blooms of picoplanktonic cyanobacterium Synechococcus in Florida Bay, a
495 subtropical inner-shelf lagoon. Limnol. Oceanogr., 44, 1166–1175, 1999.

Pierrot, D., Neill, C., Sullivan, K., Castle, R., Wanninkhof, R., Lüger, H., ... and& Cosca, C. E.: Recommendations for autonomous underway pCO2 measuring systems and data-reduction routines,. Deep Sea Research Part II: Topical Studies in Oceanography,. 56(8-10), 512-522, 2009.

Prager, E. J., and Halley, R. B.: The influence of seagrass on shell layers and Florida Bay mudbanks,. Journal of Coastal
500 Research 15: 1151–1162, 1999.

Raymond, P. A., and Cole, J. J.: Gas exchange in rivers and estuaries: choosing a gas transfer velocity, Estuaries, 24, 269–274, doi:10.2307/1352954, 2001.

Saltzman, E. S., King D. B., Holmen, K., and Leck, C.: Experimental determination of the diffusion coefficient of dimethylsulfide in water, J. Geophys. Res., 98:16481-16486, doi:10.1029/93JC01858, 1993.

505 Schorn, S., Ahmerkamp, S., Bullock, E., Weber, M., Lott, C., Liebeke, M., ... and Milucka, J.: Diverse methylotrophic methanogenic archaea cause high methane emissions from seagrass meadows, Proceedings of the National Academy of Sciences, 119(9), e2106628119, 2022.

Sharqawy, M. H., Lienhard, J. H., & Zubair, S. M.: Thermophysical properties of seawater: a review of existing correlations and data, Desalination and water treatment, 16(1-3), 354-380, 2010.

510 Sogard, Powell, G. V. N., and Holmquist, J. G.: Spatial Distribution and Trends in Abundance Of Fishes Residing in Seagrass Meadows on Florida Bay Mudbanks, Bulletin of Marine Science, 44(1), 179–199, 1989.

Stauffer, R. E.: Windpower time series above a temperate lake, Limnology and Oceanography, 25(3), 513-528, 1980.

Takahashi, T., Olafsson, J., Goddard, J. G., Chipman, D. W., and Sutherland, S. C.: Seasonal variation of CO_2 and nutrients in the high-latitude surface oceans: A comparative study, Global Biogeochemical Cycles, 7(4), 843-878, 1993.

515 Van Dam, B. R., Lopes, C. C., Polsenaere, P., Price, R. M., Rutgersson, A., and Fourqurean, J. W.: Water temperature control on CO_2 flux and evaporation over a subtropical seagrass meadow revealed by atmospheric eddy covariance. Limnology & Oceanography, 66, 1–18, https://doi.org/10.1002/lno.11620, 2020.

Van Dam, B. R., Zeller, M.A., Lopes, C., Smyth, A.R., Böttcher, M.E., Osburn, C.L., Zimmerman, T., Pröfrock, D., Fourqurean, J. W., Thomas, H.: Calcification-driven CO_2 emissions exceed "Blue Carbon" sequestration in a carbonate 520 seagrass meadow, Res. Square., 10.21203/rs.3.rs-120551/v1, 2021.

Wang, J. D., van deKreeke, J., Krishnan, N., Smith, D.: Wind and tide response in Florida Bay, Bull. Mar. Sci., 54, 579–601, 1994.

Wang, J. D.: Subtidal flow patterns in western Florida Bay, Estuarine Coastal Shelf Sci., 46, 901–915, 1998.

Wanninkhof, R.: Relationship between gas exchange and wind speed over the ocean, J. Geophys. Res., 97, 7373–7381, 525 doi:10.1029/92JC00188, 1992.

Wanninkhof, R.: Relationship between wind speed and gas exchange over the ocean revisited, Limnology and Oceanography: Methods, 12(6), 351–362, https://doi.org/10.4319/lom.2014.12.351, 2014.

Wanninkhof, R., and Thoning, K.: Measurement of fugacity of CO2 in surface water using continuous and discrete sampling methods, Mar. Chem., 44, 189–205, 1993.

530 Wanninkhof, R., Ledwell, J. R., Broecker, W. S., & Hamilton, M.: Gas exchange on Mono Lake and Crowley Lake, California, Journal of Geophysical Research, 92, 14,567–14,580, https://doi.org/10.1029/JC092iC13p14567, 1987.

Wanninkhof, R., Asher, W., Weppernig, R., Chen, H., Schlosser, P., Langdon, C., and Sambrotto, R.: Gas transfer experiment on Georges Bank using two volatile deliberate tracers, J. Geophys. Res., 98, 20,237–20,248, 1993.

Wanninkhof, R., Asher, W. E., Ho, D. T., Sweeney, C., and McGillis, W. R.: Advances in quantifying air-sea gas exchange

535   and environmental forcing, Annu. Rev. Mar. Sci., 1, 213–244, doi:10.1146/annurev.marine.010908.163742, 2009.

Weiss, R. F.: Carbon dioxide in water and seawater: The solubility of a nonideal gas, Mar. Chem., 2, 203–215, 1974.

Wilke, C. R., and Chang, P.: Correlation of diffusion coefficients in dilute solutions, AIChE Journal, 1(2), 264–270, https://doi.org/10.1002/aic.690010222, 1955.

Yates, K. K., Dufore, C., Smiley, N., Jackson, C., and Halley, R. B.: Diurnal variation of oxygen and carbonate system

540   parameters in Tampa Bay and Florida Bay, Mar. Chem., 104, 110–124, doi: 10.1016/j.marchem.2006.12.008, 2007.

Zhang, J.-Z., and Fischer, C. J.: Carbon dynamics of Florida Bay: Spatiotemporal patterns and biological control, Environ. Sci. Technol., 48: 9161−9169, doi:10.1021/es500510z, 2014.

Zheng, M., De Bruyn, W. J., and Saltzman. E. S.: Measurements of the diffusion coefficients of CFC-11 and CFC12 in pure water and seawater, J. Geophys. Res., 103:1375- 1379, doi:10.1029/97JC02761, 1998.

545   Zieman, J. C., Fourqurean, J. W., and Iverson, R. L.: Distribution, abundance and productivity of seagrasses and macroalgae in Florida Bay, Bull. Mar. Sci., 44: 292–311, 1989.

Zieman, J. C., Fourqurean, J. W., and Frankovich, T. A.: Seagrass die-off in Florida Bay: long-term trends in abundance and growth of turtle grass, Thalassia testudinum, Estuaries, 22(2), 460-470, 1999.